

Analysis of Intramolecular Dynamic Processes in Enantiomeric Diaryl Atropisomers and Related Derivatives by ^2H NMR Spectroscopy in Polypeptide Liquid Crystals

Olivier Lafon,^[a] Philippe Lesot,^{*[a]} Chun-An Fan,^[b] and Henri B. Kagan^[b]

Abstract: We demonstrate the analytical potential of ^2H - $\{^1\text{H}\}$ NMR spectroscopy in weakly ordering, chiral lyotropic liquid crystals made of poly(γ -benzyl-L-glutamate) (PBLG) dissolved in chloroform or dichloromethane for investigating the intramolecular dynamic processes of four deuterated diaryls (derivatives of 1-(4'-methylphenyl)-naphthalene). When the rotation of the aryl groups about the sp^2 - sp^2 bond is sufficiently slow relative to the NMR timescale, the method allows the spectral discrimination of enantiomeric atropisomers or enantiotopic directions in the prochiral derivatives. The effect of the position of substituents on the phenyl group on the conformational dynamics of these compounds has been examined as well as the nature of the organic co-solvent. When coalescence

phenomena are observed, simulation of the experimental ^2H - $\{^1\text{H}\}$ lineshapes using a formalism tailored for two deuterons undergoing mutual exchange allows the rate constants and the activation parameters for the internal rotation processes to be calculated. Experimental values of ΔH^\ddagger have been compared with data evaluated by molecular modelling calculations and the activation parameters are discussed for the various compounds. It is shown that these polypeptide mesophases have no significant impact on the interconver-

sion dynamics of these compounds. In contrast with the nematic thermotropic phases, Haller's equation cannot be used to predict the evolution of the quadrupolar splittings ($\Delta\nu_{\text{Q}}$ values), and hence the order parameters, versus T in the PBLG mesophases. For these particular lyotropic systems, it is shown that an exponential function of the form $\Delta\nu_{\text{Q}}[\text{Hz}] = C \times \exp(-E/RT[\text{K}])$ provides excellent agreement between the experimental and expected $\Delta\nu_{\text{Q}}$ values. Analysis of the results reported in this work suggests that orientation and chiral discrimination phenomena in these lyotropic solvents could be treated separately because they would involve different interaction mechanisms.

Keywords: atropisomerism • chirality • conformational analysis • exchange processes • kinetic and activation parameters • liquid crystals • NMR spectroscopy

Introduction

The use of chiral atropisomers in asymmetric synthesis has successfully been investigated during the last two decades.^[1,2] Atropisomerism is a particular class of stereoisomerism involving molecular structures in which internal ro-

tation about a single covalent bond is sufficiently hindered such that different stereoisomers can be isolated.^[1-3] Typical examples are tetra-*ortho*-substituted diaryls. In these compounds, the bulkiness of the substituents determines the height of the barrier to the rotation about the sp^2 - sp^2 single bond that corresponds to the activation energy for the interconversion between the enantiomeric or diastereoisomeric atropisomers. The ability to separate their signals using chromatographic techniques (HPLC, GC) or NMR spectroscopy is directly related to the exchange rate constant, that itself depends on the magnitude of the barrier to rotation, ΔH^\ddagger , and the sample temperature, T .

NMR spectroscopy is exquisitely well-suited to the analysis of dynamic phenomena (tautomerism, hindered rotation, etc.). The method relies on the fact that dynamic processes modify the resonance lineshapes when the exchange or interconversion rate constant, k , is comparable to the magni-

[a] Dr. O. Lafon, Dr. P. Lesot
Laboratoire de Chimie Structurale Organique
ICMMO UMR CNRS 8182
Bât. 410, Université de Paris-Sud, 91405 Orsay (France)
Fax: (+33)169-15-81-05
E-mail: philesot@icmo.u-psud.fr

[b] Dr. C.-A. Fan, Prof. H. B. Kagan
Laboratoire de Catalyse Moléculaire, ICMMO UMR CNRS 8182
Bât. 420, Université de Paris-Sud, 91405 Orsay (France)

Supporting information for this article is available on the WWW under <http://www.chemeurj.org/> or from the author.

tude of the NMR interactions (in frequency units).^[4,5] In isotropic NMR methods, only the isotropic part of the chemical shift or scalar coupling provides information on the dynamic processes,^[4,5] even though original approaches involving diffusion NMR experiments (DOSY spectroscopy) have recently been explored.^[6] This restriction can limit the efficiency of the method if the dynamic process does not sufficiently affect NMR interactions and thereby modify the NMR spectra. To overcome this problem, the use of NMR spectroscopy in magnetically aligned media was proposed in the early seventies.^[7-9] In particular, proton-decoupled deuterium NMR (²H-¹H} NMR) spectroscopy of isotopically enriched compounds embedded in liquid crystals (LCs) was successfully applied to the analysis of various types of dynamic processes.^[7,8]

Although the molecules under investigation have to be isotopically labelled, the analysis of molecular interconversion processes using ²H-¹H} NMR spectroscopy of deuterated molecules in liquid crystals possesses several practical advantages.^[7,8] Firstly, the spectra are free of background signals originating from the LC. Secondly, the dynamic effects on the NMR lineshapes and the coalescence phenomena can be readily interpreted because the spectra are only dominated by residual quadrupolar interactions. Thirdly, the spectral separations between exchanging ²H anisotropic signals can be much larger than those observed in isotropic ¹H or ¹³C NMR spectra, thus allowing a much wider

range of dynamic processes to be studied.^[7,8] Fourthly, the simulation of dynamic ²H-¹H} NMR spectra requires only the solution of Bloch-McConnell-type equations rather than the full density matrix^[9] and so calculations of the kinetic rate constants and activation parameters are facilitated.

Until now such investigations were restricted to molecules dissolved in achiral thermotropic nematics such as EBBA, phase V or ZLI 2452.^[9-12] In particular, the method was used to study the ring inversion of perdeuterated (halo)cyclohexanes,^[9,11] *p*-dioxane,^[12] and *cis*-decalin.^[10] However, this approach should basically be irrelevant in the analysis of interconversions between enantiomers or enantiotopic directions because their spectral discrimination is impossible in an achiral LC. To overcome this problem, it is necessary to record ²H NMR spectra using chiral liquid crystals (CLCs), such as those made of poly(γ -benzyl-L-glutamate) (PBLG) dissolved in chloroform or dichloromethane.^[13-17] In these

chiral LCs, enantiomers or enantiotopic directions in prochiral molecules are on average oriented differently and hence their residual anisotropic magnetic interactions are likely to be different.^[15,16,18]

Very recently, we reported the first example of the analysis of rotational isomerism phenomena using NMR spectroscopy in CLCs.^[19] In this work, we extensively explore the analytical potential of ²H NMR spectroscopy in polypeptide mesophases for the investigation of the intramolecular dynamic process of four deuterated diaryls derived from 1-(4'-methylphenyl)naphthalene and denoted **1-4**. The structures and the numbering are given in Figure 1. From a stereo-

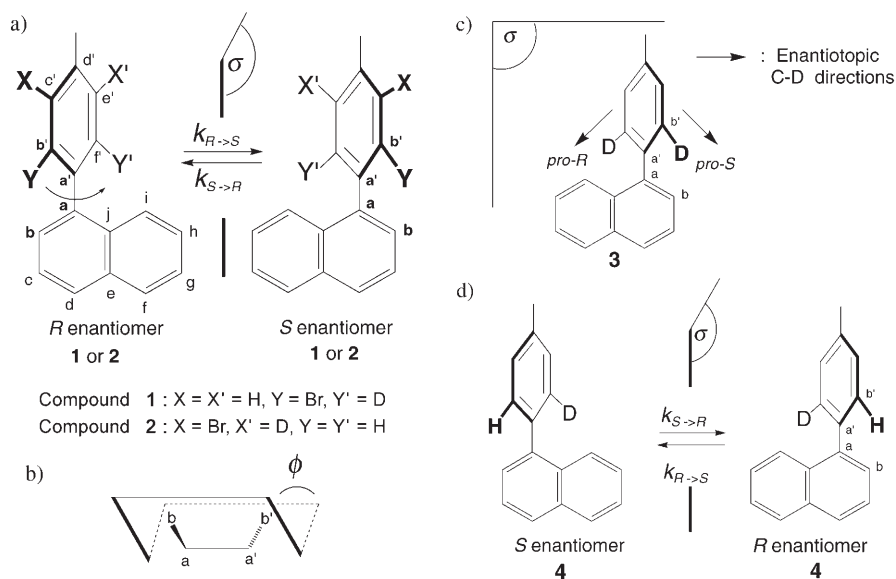


Figure 1. a) Enantiomeric conformers associated with the 1-bromo-3-deuterio-5-methyl-2-(1'-naphthyl)benzene (**1**) and the 1-bromo-3-deuterio-2-methyl-5-(1'-naphthyl)benzene (**2**). The absolute configuration of each enantiomer is defined by application of the Cahn-Ingold-Prelog priority rules.^[3] The notation (a-j and a'-g') applies to all compounds. b) Definition of the inter-ring torsion angle (b - a - a' - b'), ϕ , used to calculate the potential energy profiles. c) Elements of symmetry for 1-(2',6'-dideuterio-4'-methylphenyl)naphthalene (**3**) when the dihedral angle, ϕ , is equal to 90°. In this case, the C-D directions are enantiotopic. d) Enantiomeric rotamers associated with 1-(2'-deuterio-4'-methylphenyl)naphthalene (**4**).

chemical point of view, the monobromide aromatic derivatives, **1** and **2**, are chiral compounds for non-planar conformations. On the other hand, the non-planar, di- and mono-deuterated derivatives, **3** and **4**, can be defined as prochiral and chiral by virtue of the isotopic substitution H/D, respectively.

In an introductory part, we will briefly present some aspects of dynamic ²H NMR spectroscopy in CLCs. Then the discussion will be divided into three subsections. Firstly, we will analyse the conformational behaviour of compounds **1-4** using molecular modelling calculations (MMCs). Secondly, the ²H NMR results in PBLG mesophases will be presented. In particular, we will examine the influence of the position of bromine and deuterium atoms on the barrier to rotation. Thirdly, we will investigate the effect of organic co-solvents on the conformational dynamics of these biaryls. For all compounds, the activation parameters (ΔH^\ddagger , ΔS^\ddagger and

$\Delta G^\ddagger(T)$ will be determined by ^2H NMR spectroscopy in CLCs or by other methods such as HPLC and subsequently compared with those predicted by MMCs.

Theoretical Aspects

Enantiodiscrimination using ^2H NMR in chiral liquid crystals: In deuterium (spin $I=1$) NMR spectroscopy using liquid crystals as solvent, the partially averaged magnetic interactions are dominated by the quadrupolar interaction.^[20,21] The ^2H - $\{^1\text{H}\}$ NMR spectra of deuterated solutes or of solutes at the natural abundance level consist of the sum of quadrupolar doublets in accord with the number of non-equivalent deuterons.^[16] In CLCs, the existence of enantioselective interactions leads enantiomers or enantiotopic directions (for instance C–D bonds) in prochiral molecules to be oriented differently on average, and hence S^R or $pro\text{-}R \neq S^S$ or $pro\text{-}S$, where S is an order parameter [see Eq. (2)].^[13,16] Clearly, NMR analysis of these systems provides information that is not accessible by NMR analysis in achiral LCs. Enantiodifferentiation observed in ^2H - $\{^1\text{H}\}$ NMR spectra is based on differences between the quadrupolar splittings, $|\Delta\nu_Q^A - \Delta\nu_Q^B|$, expressed in Hz, where the subscripts A and B correspond to the stereochemical descriptors R and S for enantiomers and $pro\text{-}R$ and $pro\text{-}S$ for enantiotopic directions. In both cases, the quadrupolar splittings are given by Equation (1),^[14,15,21] where K_D is the ^2H quadrupolar coupling, $S_{C-D}^{A \text{ or } B}$ is the internuclear order parameter associated with the C–D bond, given by Equation (2), and $\theta_{C-D}^{A \text{ or } B}$ is the angle between the C–D axis and the magnetic field axis.^[14,15] In practice, when S_{C-D}^A differs from S_{C-D}^B , then two sharp quadrupolar doublets centred generally on the same chemical shift (small ^2H chemical shift anisotropy) are observed (Figure 2).^[14,15] The relatively large magnitude of the K_D parameter (160–185 kHz) contributes to the success of the method.

$$\Delta\nu_Q^{A \text{ or } B} = \frac{3}{2} K_D S_{C-D}^{A \text{ or } B} \quad (1)$$

$$S_{C-D}^{A \text{ or } B} = \left\langle \frac{3\cos^2(\theta_{C-D}^{A \text{ or } B}) - 1}{2} \right\rangle \quad (2)$$

Dynamic NMR spectroscopy of spin $I=1$ nuclei and activation parameters:

The theory of dynamic ^2H NMR spectroscopy in oriented solvents has been described by various authors.^[7,22] For our purpose, we restricted the framework to two non-coupled, non-equivalent deuterons in mutual interconversion (denoted A and B) and undergoing only Zeeman and quadrupolar interactions. In our case the two sites will correspond to either enantiomers ($A, B \equiv R$ or S) or enantiotopic directions ($A, B \equiv pro\text{-}R$ or $pro\text{-}S$) and an exchange process between two “equally populated sites” only is considered.^[23] Owing to the absence of a difference in the chemical shift between the exchanging sites ($\omega_0^A = \omega_0^B = \omega_0$), the positions of the two transitions ($\omega_{0,1}$ and $\omega_{-1,0}$) are locat-

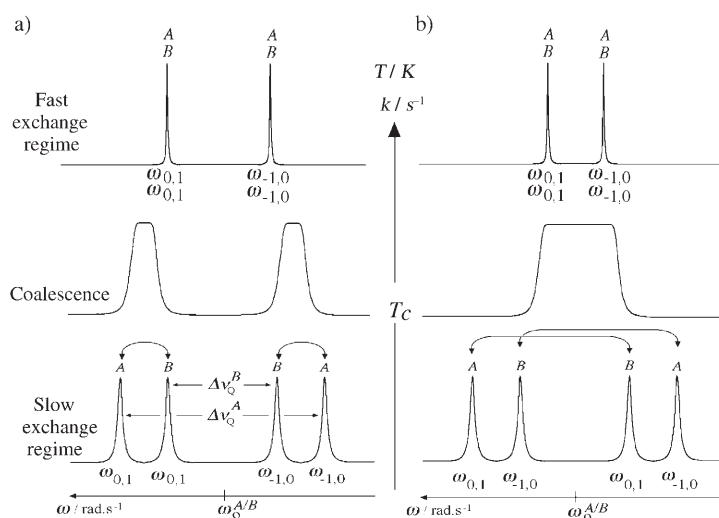


Figure 2. a) Schematic structures of 1D ^2H NMR spectra of two deuterons (A and B) undergoing mutual exchange in the three possible exchange regimes. We assume that the signs of $\Delta\nu_Q^A$ and $\Delta\nu_Q^B$ are positive, $|\Delta\nu_Q^A| > |\Delta\nu_Q^B|$, and $|\Delta\nu_Q^A| - |\Delta\nu_Q^B|$ is smaller than $|\Delta\nu_Q^A|$ and $|\Delta\nu_Q^B|$. b) Identical to a) but for $\Delta\nu_Q^A > 0$ and $\Delta\nu_Q^B < 0$. The arrows indicate the mutually exchanged transitions. The reduction of both $\Delta\nu_Q$ values and linewidths at high temperature mimics the decrease in orientational order when T is increased.

ed symmetrically relative to the offset resonance frequency, ω_0 , irrespective of the sign of the quadrupolar splittings, as shown in Figure 2. Readers interested in the theoretical formalism used in this work can refer to the Supporting Information.

Computer simulation of the ^2H NMR spectral lineshapes and their fits with experimental resonances allow the kinetic constant, k , at the various temperatures explored to be determined. However, as the kinetic rate constant, the quadrupolar splittings and the relaxation time of deuterons are temperature-dependent, an accurate determination of k from simulations requires a good assessment of the parameters $\Delta\omega = 2\pi(\Delta\nu_Q^A/2 - \Delta\nu_Q^B/2)$ and $1/T_2^*$ at each temperature (see the Supporting Information).^[7–9,24] Nevertheless, sufficiently accurate values of $1/T_2^*$ can be inferred from the linewidths of analogous samples (at the same T) in which exchange is not observed (achiral mesophase). If the difference, $\Delta\omega$, is directly measured from ^2H NMR spectra in the slow exchange regime, the $\Delta\omega$ values in the fast exchange regime will be obtained by extrapolation of the evolution of $\Delta\nu_Q$ values in the slow exchange regime, as we will describe in the discussion below.^[12,24]

In a second step, the set of k parameters extracted from simulated ^2H NMR spectra is analysed by plotting an Eyring's plot, namely the natural logarithm of kNh/RT against $1/T$, before and after the coalescence temperature (see Figure 6b).^[5a] Indeed, the dependence of $k(T)$ on temperature is theoretically described by Eyring's Equation (3),^[25,26] where ΔG^\ddagger is defined by Equation (4), $R = 8.31 \text{ J K}^{-1} \text{ mol}^{-1}$, $N = 6.02 \times 10^{23} \text{ mol}^{-1}$ and $h = 6.62 \times 10^{-34} \text{ J s}$.

$$k(T) = \frac{RT}{Nh} \exp\left(-\frac{\Delta G^\ddagger}{RT}\right) \quad (3)$$

$$\Delta G^\ddagger(T) = \Delta H^\ddagger - T\Delta S^\ddagger \quad (4)$$

Interestingly, the rate constant, $k(T_c)$ (in s^{-1}), and the free energy of activation at the coalescence temperature T_c , $\Delta G^\ddagger(T_c)$ (in kJ mol^{-1}), can be rapidly deduced from the measurement of the half-difference of values of $|\Delta\nu_Q|$ ($|\Delta\Delta\nu_Q/2| = |\Delta\nu_Q^A/2 - \Delta\nu_Q^B/2|$) in the ^2H NMR spectra below T_c .^[27] Indeed, at this particular temperature and assuming identical T_2^* for both exchanging deuterons, we can write Equations (5) and (6).^[2,3,5a,25]

$$k(T_c) = \frac{2\pi \times |\Delta\nu_Q^A/2 - \Delta\nu_Q^B/2|}{2\sqrt{2}} \quad (5)$$

$$\Delta G^\ddagger(T_c) = RT_c \times \ln\left(\frac{RT_c}{Nh} \times \frac{\sqrt{2}}{\pi \times |\Delta\nu_Q^A/2 - \Delta\nu_Q^B/2|}\right) \quad (6)$$

Results and Discussion

Conformational analysis of diaryl derivatives 1–4 by MMCs:

We have determined the evolution of the potential energy, E_{pot} , of **1–4** as a function of the inter-ring dihedral angle, ϕ (b-a-a'-b'), by MMCs (see Figure 1b). The calculations were carried out with the Hyperchem 5.0 software package using the semi-empirical AM1 force field.^[28,29] More sophisticated approaches such as ab initio (STO-3 G) or DFT methods^[30] were not used because the relative energies obtained with the AM1 and STO-3G methods for some specific values of ϕ differed by less than 3%. Hence it was pertinent to plot $E_{\text{pot}} = f(\phi)$ by using the less time-consuming method. Owing to the Born–Oppenheimer's approximation, the classical quantum-chemical software packages are not able to take into consideration isotope effects and hence they cannot distinguish between hydrogen and deuterium atoms. To mimic the decrease in the average distance of a C–D bond, we have artificially shortened the C–H distance to 107.3 pm at the site of isotopic substitution.^[31]

The results of the MMCs are discussed in two parts. First, we compare the potential energy profiles of diaryl bromide derivatives **1** and **2**, which are both chiral with non-planar geometries (see Figure 1a) but differ from each other by virtue of the position of the bromine atom in the methylphenyl group. The different positions of the bromine atom in **1** and **2** should affect the height of the barrier to internal rotation about the a–a' bond. Hence, the characteristics of the ^2H NMR spectra in chiral LCs should be significantly modified in terms of chiral discrimination at a given temperature, for instance, at room temperature. Secondly, we discuss the case of di- and monodeuterated derivatives **3** and **4** to analyse the effect of isotopic (H/D) substitution on conformational exchange.

The evolution of E_{pot} for **1** and **2** between 0 and 360° is displayed in Figure 3. For a simple comparison of data, the maximum for each curve has been set to 0. Data relative to these plots are listed in Table 1. For **1** and **2**, the curves are

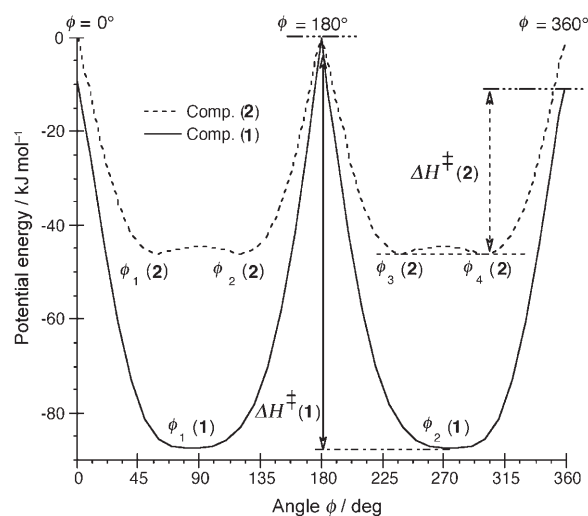


Figure 3. Potential energy profiles of **1** and **2** versus the dihedral angle ϕ (0–360°). The maximum for each curve was set to 0.

Table 1. Data extracted from the potential energy profile analysis of compounds **1–4**.

Compound	$\phi_{\text{min}}^{\text{[a]}}$ [°]	$E_{\text{pot}}(0^\circ)^{\text{[b]}}$ [kJ mol $^{-1}$]	$E_{\text{pot}}(\phi_{\text{min}})^{\text{[a]}}$ [kJ mol $^{-1}$]	$E_{\text{pot}}(180^\circ)^{\text{[b]}}$ [kJ mol $^{-1}$]	$\Delta H^\ddagger^{\text{[c]}}$ [kJ mol $^{-1}$]
1	83.1	−9.4	−87.5	0	+78.1
2	57.5/ 122.5	< −0.05	−46.3	0	+46.3
3	57.5/ 122.5	< −0.05	−45.9	0	+45.9
4	57.5/ 122.5	< −0.05	−45.9	0	+45.9

[a] The minimal energy conformer was calculated by using a convergence criterion equal to 0.012 kJ mol^{-1} . [b] Each point of the curve was calculated with a convergence criterion equal to 0.04 kJ mol^{-1} . [c] Here, we define ΔH^\ddagger as being equal to $E_{\text{pot}}(0^\circ) - E_{\text{pot}}(\phi_{\text{min}})$.

symmetrical about $\phi = 180^\circ$ and the regions of the curve to the two sides of the maximum correspond to the enantiomeric conformers which may or may not be isolable, depending on the energy difference, ΔH^\ddagger , between the minimum and the maximum potential energy. In the case of **1**, steric hindrance to rotation produces the highest energy rotamer for $\phi = 180^\circ$, when the bromide interacts with the aromatic hydrogen atom denoted as i (see Figure 1). Quantitatively, the difference in E_{pot} between the maximum-energy planar rotamers obtained at $\phi = 0$ and 180° is equal to -9.4 kJ mol^{-1} . Hence, the enantiomeric interconversion process is energetically favoured when the bromine atom interacts with the aromatic hydrogen atom b ($\phi = 0^\circ$). Consequently, $\Delta H^\ddagger(\mathbf{1})$ is defined as the difference between the energy of the conformer at $\phi = 0^\circ$ and the minimum of E_{pot} .

In the case of **2**, the energies of the rotamers at $\phi=0$ (or 360°) and 180° can be considered to be equal ($<0.05 \text{ kJ mol}^{-1}$) and hence no preferential planar conformer exists. This behaviour indicates that the steric hindrance due to the bromine atom in the *meta* position is negligible compared with the steric hindrance of a bromine atom in the *ortho* position and does not affect the barrier to rotation compared with a non-substituted derivative.

The inter-ring torsion angle corresponding to the lowest energy conformation (ϕ_{min}) results from the balance between the steric repulsion due to the *ortho* substituents and the π -orbital overlap that produces maximum resonance stabilisation when the aromatic rings are co-planar.^[3] The E_{pot} curve for **1** is quite flat in the angular regions around 90 and 270° , with two minima located at $\phi_1(\mathbf{1})=83.1^\circ$ and $\phi_2(\mathbf{1})=276.9^\circ$. This pattern of behaviour is generally observed when strong steric repulsion exists between bulky *ortho* substituents.^[3] For **2**, the evolution of E_{pot} shows four local minima ($\phi_1(\mathbf{2})$, $\phi_2(\mathbf{2})$, $\phi_3(\mathbf{2})$ and $\phi_4(\mathbf{2})$) at $\phi=57.5$ and 122.5° and the complementary angles 302.5 and 237.5° . The presence of two local minima located symmetrically about 90° is due to the effect of resonance stabilisation by π orbital overlap at these four angles. This effect is measured at around 2 kJ mol^{-1} . Finally, the large difference in activation energy, ΔH^\ddagger , between **1** and **2** ($\approx 32 \text{ kJ mol}^{-1}$) originates from the difference in steric hindrance due to the bulkiness of the bromine atom (vdW radius = 185 pm) relative to the hydrogen atom (vdW radius = 120 pm).

Compared with **1** and **2**, the dideuterated compound **3** is symmetrical with two small-volume substituents on the phenyl ring (two deuterons). From a chemical point of view, this molecule can be defined as prochiral because if we are able to dissymmetrise the phenyl ring through an appropriate chemical reaction, we obtain a chiral compound for all the dihedral angles ϕ differing from 0 and 180° (planar structure).^[3] From a stereochemical point of view, this molecule is characterised by a plane of symmetry (σ) when $\phi=90^\circ$ (see Figure 1c).

Depending on the constant k , which is related to the magnitude of ΔH^\ddagger and T , the stereochemical relationship between the two C–D directions in **3** is not the same and so gives different $^2\text{H}\{-^1\text{H}\}$ anisotropic spectra. Theoretically, three stereochemical situations exist. Firstly, if the rotation around the aryl–aryl bond is fast, no spectral discrimination between the C–D directions is possible and so a single doublet is expected. Secondly, if the rotation is sufficiently hindered, the C–D directions should be distinguished if their orientational order parameters are sufficiently different in the PBLG chiral phase. As the average conformation of **3** is of C_s symmetry, the C–D directions can be considered as enantiotopic.^[3,16] In principle, two quadrupolar doublets are expected in the $^2\text{H}\{-^1\text{H}\}$ spectrum if $S_{\text{C-D}_1}^{\text{pro-R}} \neq S_{\text{C-D}_2}^{\text{pro-S}}$. Thirdly, if the rotation is impossible and if the dihedral angle ϕ is not 90° the molecule should adopt C_1 symmetry and then two enantiomeric forms exist in which the C–D directions are now diastereotopic. In this particular situation, four quadrupolar doublets should be observed. As the substituents at

the b' and f' positions are identical, the evolution of E_{pot} for **3** versus ϕ is symmetrical about $\phi=90^\circ$ and very similar to the evolution of E_{pot} for **2** (see Figure SI-2 in the Supporting Information). In fact the regions to each side of this angle correspond to enantiomeric pairs. In this particular case, it should be emphasised that the conformers at ϕ and $360-\phi$ are also mirror images and so the evolution of E_{pot} between 0 and 360° is also symmetrical about $\phi=180^\circ$. Once again, the regions to the two sides of the absolute maximum correspond to enantiomeric pairs. Steric hindrance produces the highest energy rotational conformers for $\phi=0$ (360) and 180° . Owing to the absence of stabilisation by π orbital overlap when the phenyl and naphthyl rings are orthogonal, the lowest energy conformers are not found at 90° (see Table 1).^[3] The barrier to rotation, ΔH^\ddagger , is evaluated as $+45.9 \text{ kJ mol}^{-1}$, while the barrier to interconversion between the enantiomeric conformer pairs, ϕ_1/ϕ_2 or ϕ_3/ϕ_4 , is less than $+2 \text{ kJ mol}^{-1}$. The slightly smaller value of ΔH^\ddagger for **3** relative to **2** (0.4 kJ mol^{-1}) indicates that the bromine atom in the *meta* position has only a very small effect on the height of the barrier to rotation.

As a result of dissymmetrisation of the phenyl ring, the diaryl **4** does not possess a plane of symmetry for the conformation $\phi=90^\circ$ and it can be defined as a chiral derivative by virtue of the isotopic substitution (H/D). This molecule presents enantiomeric forms when ϕ is different to 0 and 180° . In the past, some rigid and flexible chiral molecules due to isotopic substitution have been investigated by ^2H NMR spectroscopy in polypeptide LCs, but derivatives exhibiting a conformational exchange detectable by NMR spectroscopy have not yet been explored.^[32,33] In addition, it is worthwhile comparing the results obtained for **3** and **4** in order to analyse possible steric isotope effects on ^2H NMR spectra.^[34] The MMCs carried out on **4** show that the potential energy profiles for **3** and **4** are identical. No deviation of the ϕ angles or of the ΔH^\ddagger values for **3** and **4** occurs when one of two C–D bonds is replaced by a C–H bond in the structure.

NMR study of 1-bromo-3-deuterio-5-methyl-2-(1'-naphthyl)-benzene (1): The $^2\text{H}\{-^1\text{H}\}$ NMR spectrum of compound **1** dissolved in PBLG/ CHCl_3 at room temperature shows two quadrupolar doublets with a difference in quadrupolar splittings, $|\Delta\nu_{\text{Q}}^A - \Delta\nu_{\text{Q}}^B|$, equal to 257 Hz (Figure 4a). As the absolute configuration of each doublet is unknown, the stereodescriptors *R* and *S* were replaced by the arbitrary notations *A* and *B*. The presence of two doublets suggests a priori a difference in the orientation of the C–D direction in each enantiomer. To confirm this, we recorded the $^2\text{H}\{-^1\text{H}\}$ NMR spectrum of **1** dissolved in an achiral polypeptide oriented phase made of an equimassic mixture of PBLG and PBDG (enantiomer of PBLG), both dissolved in CHCl_3 (see Table 4 below). In this mixture, denoted "PBG", the spectral discrimination of the enantiomers or enantiotopic directions was eliminated.^[35] Experimentally, the two doublets collapse into a single doublet. This second step therefore shows unambiguously that the enantiomers of **1** are spectrally dis-

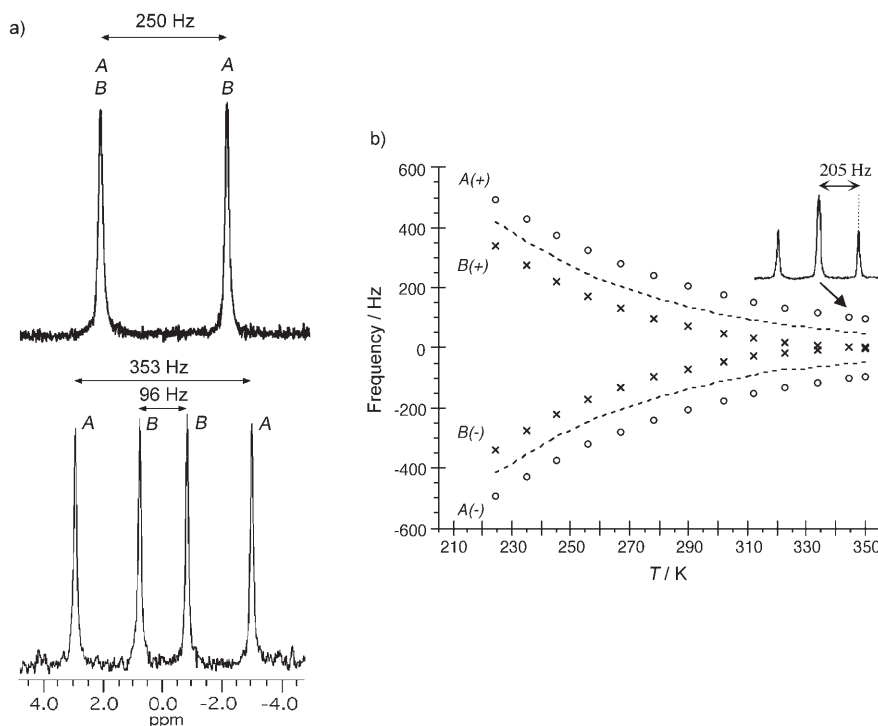


Figure 4. a) 61.4 MHz $^2\text{H}\{-^1\text{H}\}$ NMR spectra of **1** recorded at $T=302$ K in the PBG/ CHCl_3 achiral phase (top) and in the PBLG/ CHCl_3 chiral phase (bottom). b) Graphical evolution of positive and negative components of doublets *A* (outer) and *B* (inner) of **1** in the PBLG/ CHCl_3 phase versus T . The dashed line corresponds to an experimental value of $\Delta\nu_{\text{Q}}^{\text{average}}$, namely the evolution that should be observed in the achiral mesophase assuming the same sign for values of $\Delta\nu_{\text{Q}}$. The insert shows the spectrum recorded at 345 K.

criminated. If this was not the case, two doublets would still be observed in PBG and then the NMR spectra in the two mesophases would be accounted for by other reasons (molecular conformational effects or mesophase-related phenomena). The magnitude of the doublet splitting in the PBG mesophase ($|\Delta\nu_{\text{Q}}^{\text{PBG}}|=250$ Hz) implies that the sign of the quadrupolar splittings in PBLG are identical, either positive or negative. Opposite signs would have led to a value of around 130 Hz. Ideally, the anticipated value should be equal to 225 Hz, but differences in the sample preparation can yield these small differences (see below). Finally, note that enantiomers of **1** have also been discriminated by proton-decoupled ^{13}C NMR spectroscopy.^[14,36] Remarkably, this example illustrates that NMR spectroscopy in CLCs can be used to analyse chiral molecules without any stereogenic centre and devoid of conventional reactive functionality for which classical NMR tools are rather limited.^[15]

From a conformational analysis point of view, we show here that the interconversion between enantiomers of **1** is sufficiently slow on the ^2H NMR timescale to allow separation of their deuterium signals at room temperature. This result is consistent with the ΔH^\ddagger value calculated by MMCs. Within experimental error, integration of the peak areas of *A* and *B* leads to identical values, thus indicating that the mixture is still racemic in the chiral LC phase. This implies that $K=k_{R\rightarrow S}/k_{S\rightarrow R}=1$ and thus shows that the mesophase

does not modify the equilibrium constant in favour of one of the two enantiomers.

In a second series of NMR experiments, we recorded the $^2\text{H}\{-^1\text{H}\}$ NMR spectra of **1** versus T (224–350 K) to check if the coalescence phenomenon could be observed (see Figure 4b). The evolution of the difference in quadrupolar splittings, $|\Delta\nu_{\text{Q}}^{\text{A}}-\Delta\nu_{\text{Q}}^{\text{B}}|$, the average linewidth (measured on the four components) and the average quadrupolar splitting, $\Delta\nu_{\text{Q}}^{\text{average}}=|\Delta\nu_{\text{Q}}^{\text{A}}+\Delta\nu_{\text{Q}}^{\text{B}}|/2$, is provided in the Supporting Information (see Figure SI-3). Analysis of the spectra shows that enantiomers are differentiated over the entire range of T . This result also includes the case in which one singlet and one doublet are simultaneously observed, as in the spectrum recorded at $T=345$ K (see the inset in Figure 4b). This situation arises when the C–D internuclear axis of one of the two enantiomers is aligned on average along the magic angle ($\theta=$

54.7°) direction [Eq. (2)]. As a consequence, even at very high temperatures, the coalescence phenomenon was not observed.

As expected for any solute in a LC, the quadrupolar splittings increase monotonically as T decreases. This is a consequence of the reduction in the mobility of molecules in the mesophase as T is lowered. For a simple quantitative evaluation of the evolution of $|\Delta\nu_{\text{Q}}^{\text{average}}|$, $|\Delta\nu_{\text{Q}}^{\text{A}}|$, $|\Delta\nu_{\text{Q}}^{\text{B}}|$ or $|\Delta\nu_{\text{Q}}^{\text{A}}-\Delta\nu_{\text{Q}}^{\text{B}}|$ versus T , we can calculate the relative spectral variation, $\Delta X/\bar{X}$, expressed in %, of these quantities between T_{min} and T_{max} by using Equation (7), where X represents $|\Delta\nu_{\text{Q}}^{\text{average}}|$, $|\Delta\nu_{\text{Q}}^{\text{A}}|$, $|\Delta\nu_{\text{Q}}^{\text{B}}|$ or $|\Delta\nu_{\text{Q}}^{\text{A}}-\Delta\nu_{\text{Q}}^{\text{B}}|$. From this simple evaluation, we find that the relative spectral variations of $|\Delta\nu_{\text{Q}}^{\text{A}}-\Delta\nu_{\text{Q}}^{\text{B}}|$ and $|\Delta\nu_{\text{Q}}^{\text{average}}|$ between T_{min} and T_{max} are equal to 38 and 160 %, respectively. This large difference in the relative variation of these quantities suggests that chiral discrimination and orientation mechanisms are two separate phenomena. This assumption is supported by other results reported in this paper.

$$\frac{\Delta X}{\bar{X}} [\%] = 100 \times \frac{X^{T_{\text{max}}} - X^{T_{\text{min}}}}{(X^{T_{\text{max}}} + X^{T_{\text{min}}})/2} \quad (7)$$

The evolution of $|\Delta\nu_{\text{Q}}^{\text{average}}|$ (and associated order parameters) as well as $|\Delta\nu_{\text{Q}}^{\text{A}}|$ and $|\Delta\nu_{\text{Q}}^{\text{B}}|$ versus T (in K) over a range of around 130 K can be fitted using an exponential

function of the form given by Equation (8), where $R = 8.314 \text{ J K}^{-1} \text{ mol}^{-1}$ and the constants C and E are the parameters to be evaluated. Values of C and E are expressed in Hz and J mol^{-1} , respectively, and are listed in Table 2.

$$\Delta\nu_{\text{O}}[\text{Hz}] = C \times \exp\left(-\frac{E}{RT[\text{K}]}\right) \quad (8)$$

Table 2. C and E parameters for fitting the evolution of $|\Delta\nu_{\text{O}}^{\text{average}}|$, $|\Delta\nu_{\text{O}}^{\text{A}}|$ and $|\Delta\nu_{\text{O}}^{\text{B}}|$ using Equation (8).

Entry	Compd	Polypeptide/ co-solvent	C prefactor	E factor	Average E factor	χ parameter
			[Hz]	[kJ mol ⁻¹]		
			$ \Delta\nu_{\text{O}}^{\text{average}} $	$ \Delta\nu_{\text{O}}^{\text{A}} $	$ \Delta\nu_{\text{O}}^{\text{A}} / \Delta\nu_{\text{O}}^{\text{B}} $	
			$ \Delta\nu_{\text{O}}^{\text{A}} / \Delta\nu_{\text{O}}^{\text{B}} $	$ \Delta\nu_{\text{O}}^{\text{A}} / \Delta\nu_{\text{O}}^{\text{B}} $		
1	1	PBLG/CHCl ₃	4.43	-9.866	-10.758	0.992
	1	PBLG/CH ₂ Cl ₂	15.1/0.49	-7.881/-13.635	-8.709	0.981/0.995
			9.43	-8.253		0.999/0.995
3	2	PBLG/CHCl ₃	21.2/2.1	-7.347/-10.071	-3.585	0.999/0.995
			128.3	-3.583		0.999
4	3	PBLG/CHCl ₃	204.4/77.6	-3.063/-4.108	-4.081	0.997/0.999
			81.7	-4.337		0.998
5	3	PBLG/CHCl ₃	143.6/59.6	-3.493/-4.668	-	0.997/0.996
			82.3	-4.442		0.998
6	3	PBLG/CH ₂ Cl ₂	121.9	-2.272	-1.299	0.996
			177.0/197.0	-2.275/-0.323	0.993/0.954	
7	4	PBLG/CHCl ₃	69.4	-4.585	-3.986	0.998
			135.8/66.4	-3.543/-4.429		0.992/0.999
8	4	PBLG/CHCl ₃	84.3 ^[b]	-4.259 ^[b]	-	0.999 ^[b]

[a] Average E factor for $|\Delta\nu_{\text{O}}^{\text{A}}|$ and $|\Delta\nu_{\text{O}}^{\text{B}}|$. [b] Corrected values for $|\Delta\nu_{\text{O}}^{\text{average}}|$ [see Eq. (9)].

The factor E is the same for fitting the evolution of $|\Delta\nu_{\text{O}}^{\text{A}}|$, $|\Delta\nu_{\text{O}}^{\text{B}}|$ or the positive, $A(+)$ or $B(+)$, and negative, $A(-)$ or $B(-)$, resonances. In contrast, the prefactor C associated with the positive and negative resonances is obtained by dividing the value of C obtained for $\Delta\nu_{\text{O}}^{\text{A}}$ or $\Delta\nu_{\text{O}}^{\text{B}}$ by a factor of +2 and -2, respectively. Except in one case (Table 2, entry 6), we observe that the outer doublet, $\Delta\nu_{\text{O}}^{\text{A}}$, is characterised by a higher C and a lower E than the inner doublet. This situation is expected if the variations in $\Delta\nu_{\text{O}}^{\text{A}}$ and $\Delta\nu_{\text{O}}^{\text{B}}$ are rather similar between T_{min} and T_{max} . Equation (8) differs from Haller's equation, $S = S_0(1 - T/T^*)^\alpha$, which is classically used to fit the evolution of the order parameters versus T for nematic liquid crystals.^[37] In fact, this equation cannot be used to fit anisotropic parameters in the case of organic solutions of PBLG because the nematic-isotropic transition temperature (N→I) cannot be determined (due to the evaporation of co-solvent). As we will see below, this kind of evolution has been ascertained using two liquid-crystalline phases irrespective of the compound (**1–4**) (see Table 2). For all of them, the factor E relative to the evolution of $|\Delta\nu_{\text{O}}^{\text{average}}|$ is approximately the average of factors E determined for $|\Delta\nu_{\text{O}}^{\text{A}}|$ and $|\Delta\nu_{\text{O}}^{\text{B}}|$. Thus, the discrepancy between the factors E obtained for **1** is less than 10%. This behaviour suggests that the enantiomeric discrimination in the CLC may be described as a deviation from the average order existing in the achiral oriented phase.

Remarkably, Equation (8) is similar to the Boltzmann's relation. In fact, we can infer that the evolution of the mag-

nitude of $\Delta\nu_{\text{O}}$ for a given C–D bond, and consequently the associated $S_{\text{C–D}}$ order parameter, versus T can be related to the "strength" of the interaction potential (van der Waals) between this molecular direction and its environment. The negative sign for E indicates an attractive potential between the PBLG helices and the C–D bond. In addition, the E values (in kJ mol^{-1}) obtained are comparable to energies associated with van der Waals interactions and are very close to the thermal energies (RT), which vary from 1.771 (213 K) to 2.910 kJ mol^{-1} (350 K) in this study.^[38] To confirm these results, further investigations on a wide range of solutes are underway.

In contrast to $|\Delta\nu_{\text{O}}^{\text{average}}|$, the variation in $|\Delta\nu_{\text{O}}^{\text{A}} - \Delta\nu_{\text{O}}^{\text{B}}|$ versus T is relatively small and its evolution can be fitted using a linear function. In this example, we found that $|\Delta\nu_{\text{O}}^{\text{A}} - \Delta\nu_{\text{O}}^{\text{B}}|$ [Hz] = $-0.934T[\text{K}] + 542.2$, with $\chi = 0.989$. The existence of distinct evolutions for $|\Delta\nu_{\text{O}}^{\text{average}}|$ and $|\Delta\nu_{\text{O}}^{\text{A}} - \Delta\nu_{\text{O}}^{\text{B}}|$ is somewhat consistent with the large differences in the relative variations of these quantities. Again, these facts are new arguments in

favour of the separation of the mechanisms for orientation and chiral discrimination, which can be seen as distinct phenomena and so treated separately.

The absence of coalescence signals at 350 K implies that T_c is at a higher temperature and hence the activation parameters cannot be calculated using 1D ²H NMR spectra in the PBLG/CHCl₃ solvent. Another co-solvent with a higher boiling point, such as DMF, could be used in order to record ²H NMR spectrum above $T = 350$ K, but this change has not been explored because the magnitude of $|\Delta\nu_{\text{O}}^{\text{A}}/2 - \Delta\nu_{\text{O}}^{\text{B}}/2|$ in this new oriented solvent is a priori unknown. To estimate the exchange rates, we have explored the use of 2D exchange spectroscopy (EXSY 2D experiments).^[22,39] However, irrespective of the mixing time used, no exchange cross-peaks between the two quadrupolar doublets were observed experimentally on the 2D map, very likely because the activation barrier is too high to be determined by this approach. In fact, because Equations (4) and (6) are equal at T_c , we may predict T_c of **1** by making some reasonable assumptions. By using the hypothesis in which the quantities $|\Delta\nu_{\text{O}}^{\text{A}}/2 - \Delta\nu_{\text{O}}^{\text{B}}/2|$ at $T > 350$ K, ΔH^\ddagger and ΔS^\ddagger are known, we can graphically resolve this equality to determine T_c and $\Delta G^\ddagger(T_c)$.^[40] The magnitude of $|\Delta\nu_{\text{O}}^{\text{A}}/2 - \Delta\nu_{\text{O}}^{\text{B}}/2|$ above 350 K can be extrapolated from the exponential fit of the entities $\Delta\nu_{\text{O}}^{\text{A}}$ and $\Delta\nu_{\text{O}}^{\text{B}}$ (see Table 2, entry 1). If the ΔH^\ddagger value can be set to the value determined by the MMCs (+78.1 kJ mol^{-1}), we ignore the ΔS^\ddagger value for **1**. However, we can assume that ΔS^\ddagger is close to the data obtained for analogous com-

Table 3. Comparison of the data evaluated by molecular modelling calculations and experimental parameters for compounds **2**, **3** and **4**.

Compd.	Data evaluated from molecular modelling		Data determined from NMR experiment in CLC							
	ϕ [°]	ΔH^\ddagger [kJ mol ⁻¹]	Polypeptide/ co-solvent	T_c [K]	$ \Delta\Delta\nu_O/2 $ [Hz]	$k(T_c)^{[a]}$ [s ⁻¹]	$\Delta G^\ddagger(T_c)^{[b]}$ [kJ mol ⁻¹]	$\Delta H^\ddagger^{[c]}$ [kJ mol ⁻¹]	$\Delta S^\ddagger^{[c]}$ [J mol ⁻¹ K ⁻¹]	$\Delta G^\ddagger(T_c)^{[c]}$ [kJ mol ⁻¹]
2	57.5/122.5	46.3	PBLG/CHCl ₃	250 ± 2	175 ± 5	389 ± 12	48.5 ± 0.5	44.7 ± 0.5	-18 ± 2	49.0 ± 0.5
3	57.4/122.6	45.9	PBLG/CHCl ₃	245 ± 2	102 ± 5	226 ± 11	48.6 ± 0.5	44.2 ± 0.5	-19 ± 2	48.9 ± 0.5
3	57.4/122.6	45.9	PBLG/CH ₂ Cl ₂	245 ± 2	106 ± 5	235 ± 11	48.5 ± 0.5	43.6 ± 0.5	-16 ± 2	47.6 ± 0.5
4	57.4/122.6	45.9	PBLG/CHCl ₃	245 ± 2	98 ± 5	218 ± 11	48.7 ± 0.5	44.3 ± 0.5	-20 ± 2	49.2 ± 0.5

[a] Values calculated from Equation (5). [b] Values calculated from Equation (6). [c] Values derived from the Eyring's plot.

pounds (such as **2**). By using this argument, the ΔS^\ddagger value was set to $-19 \text{ J mol}^{-1} \text{ K}^{-1}$ (see Table 3). This approach leads to a value for T_c of 415.5 K and $\Delta G^\ddagger(T_c)$ of $+86.0 \text{ kJ mol}^{-1}$.^[41]

As an alternative to the NMR approach, we explored the analytical potential of chiral HPLC. Thus it was possible to separate the enantiomers of **1** by using a chiral stationary phase (Chiralcel ODH column) at 298 K with hexane as eluent (flow 0.5 mL min⁻¹). The chromatogram (not shown) displays two sharp peaks (with retention time = 35.3 and 46.6 min) separated by a rather flat "plateau". These particular chromatograms are generally recorded for molecules undergoing an interconversion between enantiomers during their elution on a resolving enantiopure stationary phase. The effect is referred to as "peak coalescence of the second type".^[42] By using the technique developed by Schurig and co-workers, it is possible to simulate the chromatogram of **1** in order to evaluate $\Delta G^\ddagger(298 \text{ K}) = +91.4 \pm 0.6 \text{ kJ mol}^{-1}$.^[43] By assuming that $\Delta S^\ddagger = -19 \text{ J mol}^{-1} \text{ K}^{-1}$, we can estimate ΔH^\ddagger to be $+85.7 \text{ kJ mol}^{-1}$ from Equation (4). The difference between the data determined by this approach and that deduced by MMCs is about 10%. Although the ΔS^\ddagger term is generally small for intramolecular exchanges in small molecules, the discrepancy in ΔH^\ddagger can mainly be attributed to the approximation made for ΔS^\ddagger . Here we probably underestimate ΔS^\ddagger because **1** exhibits a much greater steric hindrance than other compounds. However, the relatively good agreement between the two results is satisfactory. Another approach would involve evaluating ΔS^\ddagger by combining the value of ΔH^\ddagger determined by MMCs and ΔG^\ddagger value derived by HPLC at 298 K. By using Equation (4) we found $\Delta S^\ddagger = -45 \text{ J mol}^{-1} \text{ K}^{-1}$. This value is two times higher than those determined by NMR analysis for **2** or **3**. By using this new value, we can evaluate T_c for compound **1** to be 473 K and $\Delta G^\ddagger(T_c)$ to be $+99.4 \text{ kJ mol}^{-1}$. Reasonably, the correct value of ΔS^\ddagger is intermediate between the two values given above. By using the average value ($-32 \text{ J mol}^{-1} \text{ K}^{-1}$), $T_c = 442.5 \text{ K}$ and $\Delta G^\ddagger(T_c) = +92.3 \text{ kJ mol}^{-1}$ are obtained.

NMR study of the 1-bromo-3-deuterio-2-methyl-5-(1'-naphthyl)benzene (2): In contrast to compound **1**, the ²H-¹H NMR spectrum of **2** recorded at room temperature (302 K) shows a single quadrupolar doublet with a splitting of 538 Hz (see Figure 5a). Consequently the interconversion between the enantiomeric forms of **2** is sufficiently fast on

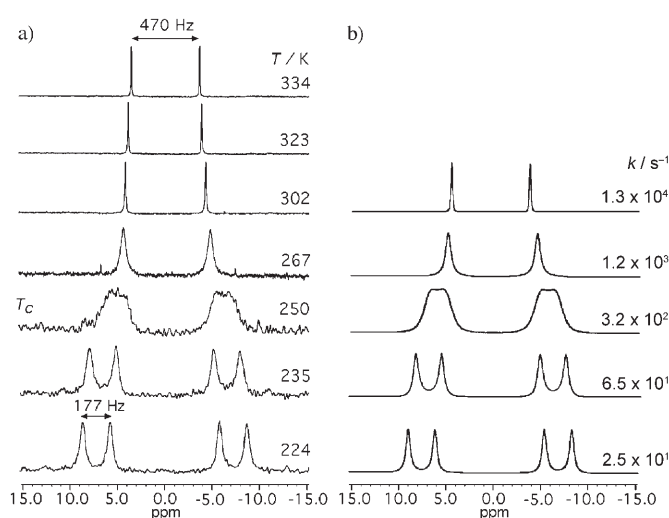


Figure 5. a) Experimental 61.4 MHz ²H-¹H NMR spectra of **2** dissolved in the PBLG/CHCl₃ phase recorded at different temperatures as indicated on the right side. b) Simulated spectra computed with the specific rate constant, k , indicated on the right side.

the NMR timescale to prevent spectral enantiodiscrimination in PBLG at room temperature. This result is in agreement with the smaller barrier to internal rotation in **2** relative to **1**, as evaluated by MMCs (see Table 1). Spectrally, this single quadrupolar doublet corresponds to the average of the quadrupolar splittings arising from the *R* and *S* isomers. In fact, this ²H NMR spectrum is identical to that expected in the achiral oriented solvent, PBG. This conclusion will be illustrated for diaryl **3**.

To observe the coalescence phenomenon for **2**, we have to reduce the interconversion rate by lowering the temperature. Figure 5a shows the experimental evolution of the anisotropic ²H-¹H NMR spectra of **2** versus T . For a better visualisation, the evolution of $\Delta\nu_O$ values over the temperature range 224–350 K is shown in Figure 6a (see also Figure SI-3b in the Supporting Information). While significant line-broadening is observed below 270 K, the coalescence phenomenon occurs at $T_c = 250 \pm 2 \text{ K}$. Here, the phenomenon can be clearly identified because a single doublet with very broad components ($\approx 130 \text{ Hz}$ linewidth) is recorded. This spectral lineshape indicates that the signs of the $\Delta\nu_O$ values are the same for both enantiomers (as for **1**) at low temperatures (see Figure 2a). Thus it is possible to determine the

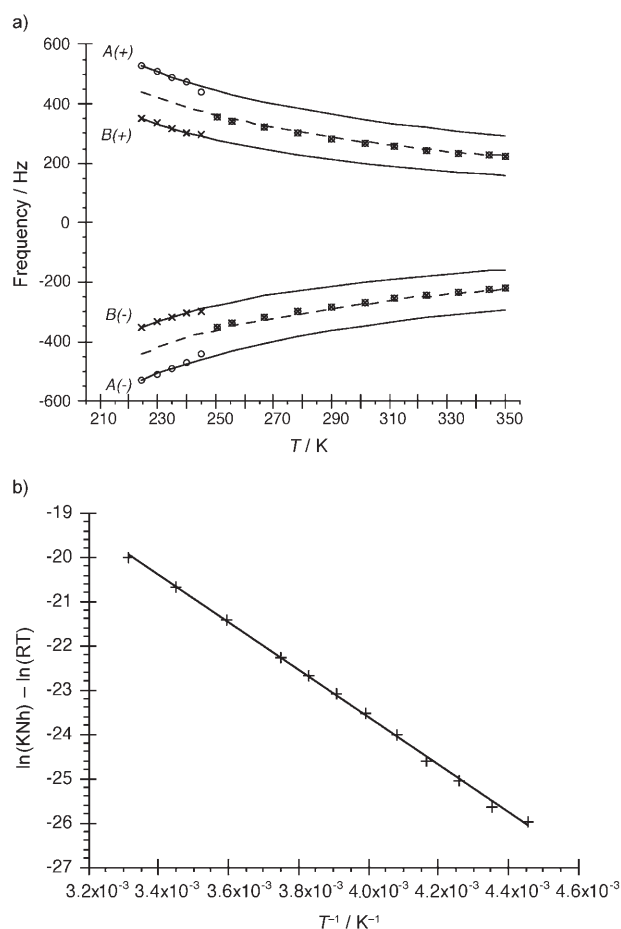


Figure 6. a) Graphical evolution of the positive and negative components of the doublets A (outer) and B (inner) of **2** dissolved in the PBLG/CHCl₃ phase versus *T*. The continuous lines represent the predicted evolution of the components for both doublets versus *T* if no coalescence phenomenon exists (see text). The dashed lines simulate the average evolution of $\Delta\nu_Q$ (derived from the predicted evolution) that should be ideally observed in the achiral oriented phase, assuming identical signs for the values of $\Delta\nu_Q$. b) Eyring's plot obtained for **2**. The full line corresponds to the linear fit of data ($\chi=0.999$).

relative sign of the $\Delta\nu_Q$ values without recording data in the PBG mesophase. Below T_c , two resolved quadrupolar doublets, the linewidths of which decrease with *T* (until 224 K), are observed, thus demonstrating that 1) the average orientation of each enantiomer is different in the mesophase and 2) their lifetime is now sufficiently long on the NMR time-scale to observe their respective NMR signal. This notable result highlights the ability of the polypeptide helices to distinguish between enantiomers of axially chiral derivatives even if the barrier to rotation is not enough to discriminate them at room temperature.

Although the half-difference of the $\Delta\nu_Q$ values is temperature-dependent, its evolution is very weak below T_c . Consequently, by adopting an average value for $|\Delta\nu_Q^A/2 - \Delta\nu_Q^B/2|$ equal to (175 ± 5) Hz, we can evaluate $k(T_c)$ to be (389 ± 12) s⁻¹ and $\Delta G^\ddagger(T_c)$ to be $(+48.5 \pm 0.5)$ kJ mol⁻¹ for **2** using Equations (5) and (6) and $T_c = (250 \pm 2)$ K. The analysis of Eyring's plot over a sufficient temperature range around T_c

allows $\Delta G^\ddagger(T_c)$ as well as other activation parameters to be calculated more accurately from NMR results. This supposes, however, that we are able to determine the rate constants for each temperature by fitting the experimental ²H NMR signals to the theoretical lineshapes [see Equations (SI-4) and (SI-5) in the Supporting Information]. Below T_c , the quantity $|\Delta\nu_Q^A/2 - \Delta\nu_Q^B/2|$ is directly measured from the experimental spectra (see Figure 5a). Above T_c , this quantity has to be extrapolated from the evolution of the A and B doublets observed in the slow exchange regime, as if the coalescence phenomenon did not exist.^[12,24] In this hypothetical case, two doublets are expected owing to chiral discrimination. Regarding the previous results obtained for **1**, we have assumed that the four transitions, $\omega_{-1,0}^A$, $\omega_{-1,0}^B$, $\omega_{0,1}^A$ and $\omega_{0,1}^B$, follow an exponential evolution over the entire temperature range. Thus, it is possible to predict the frequency evolution of these transitions versus *T* using Equation (8) and data extracted from the slow exchange regime. The parameters *C* and *E* associated with $\Delta\nu_Q^A$ and $\Delta\nu_Q^B$ values are listed in Table 2 (entry 3). As an illustration, the hypothetical evolution of the four components above T_c is shown in Figure 6a (continuous lines). Thus, these extrapolations permit the term $|\Delta\nu_Q^A/2 - \Delta\nu_Q^B/2|$ to be calculated in the fast exchange regime.^[24] By assuming that sufficiently accurate values of $1/T_2^*$ can be extracted from the linewidths of analogous samples for which no exchange process is observed (PBG phase), this strategy allows the variables of Equations (SI-4) and (SI-5) in the Supporting Information, which are actually kept constant during the fitting procedure, to be predicted.

As expected, the points on the Eyring's plot (Figure 6b) form a straight line, the slope and y intercept of which permit ΔH^\ddagger and ΔS^\ddagger , respectively, to be determined.^[5] Parameters derived from the Eyring's plot are $\Delta H^\ddagger = (+44.7 \pm 0.5)$ kJ mol⁻¹, $\Delta S^\ddagger = (-18.0 \pm 0.5)$ J mol⁻¹ K⁻¹ and finally $\Delta G^\ddagger = (+49.0 \pm 0.5)$ kJ mol⁻¹ at T_c . The discrepancy between $\Delta G^\ddagger(T_c)$ deduced from the Eyring's plot and calculated using Equation (6) mainly arises from the uncertainty in T_c . The experimental ΔH^\ddagger value differs by less than 2 kJ mol⁻¹ (<4%) from the theoretical value determined by MMCs (see Table 3), thus indicating the reliability of the two methods. The small magnitude of ΔS^\ddagger is reasonable because the transition state of small-to-medium-sized molecules undergoing an intramolecular exchange is not more significantly ordered (from the entropic point of view) than the ground state.^[5a] Under these conditions, the entropy change, ΔS^\ddagger , between the ground state (the lowest energy rotamer) and the transition state (the highest energy rotamer) is rather small or even close to zero.^[5a] Also we found that the rotation rate is around 1.3×10^4 s⁻¹ at 302 K, thus implying that spectral enantiodiscrimination could be observed at this temperature only if $|\Delta\nu_Q^A/2 - \Delta\nu_Q^B/2|$ was much larger than 5850 Hz [Eq. (5)]! Finally, the excellent agreement between the predicted and experimental ΔH^\ddagger values indicates that the intermolecular forces between the solute and the PBLG phase do not significantly influence the conformational interconversion process of **2** (compared with an isolated mole-

cule). This new study confirms other recent results involving complex calculations.^[44]

From the point of view of orientational behaviour, the comparison between the evolution of the spectral data versus T for **1** and **2** is noteworthy (see Figure 4b and Figure 6a). Indeed, as the main directions of electrical field gradient (EFG) tensor for the C–D bonds in **1** and **2** are almost parallel, they provide the same information in terms of order parameters relative to the magnetic field axis and hence it is possible to interpret the differences observed. Over the temperature range explored (224–350 K), the global evolution of $|\Delta\nu_{\text{O}}^{\text{average}}|$ and $|\Delta\nu_{\text{O}}^{\text{A}}/2 - \Delta\nu_{\text{O}}^{\text{B}}/2|$ (partly obtained by extrapolation) for **2** is similar to the evolution observed for **1**, but differences in their respective variations exist. If the relative variation of $|\Delta\nu_{\text{O}}^{\text{A}} - \Delta\nu_{\text{O}}^{\text{B}}|$ for **2** and **1** is similar (29 instead of 38%), the relative variation of $|\Delta\nu_{\text{O}}^{\text{average}}|$ is very different (67 instead of 160%). From a theoretical point of view, these results suggest that the chiral discrimination mechanisms for **2** and **1** are similar over a large temperature range and lead to spectral separation of similar magnitude. Thus the values of $|\Delta\nu_{\text{O}}^{\text{A}} - \Delta\nu_{\text{O}}^{\text{B}}|$ for **2** and **1** are equal to 314 and 353 Hz, respectively, at 213 K, and 204 and 266 Hz at 350 K. In other words, the position of the bromine atom has only a small effect on the spectral separation, thus suggesting that the discrimination mechanisms are more sensitive to a global shape recognition rather than to local changes in the molecular structure. This conclusion confirms recent work on the discrimination of chiral hydrocarbons that indicated that shape recognition plays a crucial role in the chiral discrimination mechanisms of apolar enantiomers.^[15] In contrast, the molecular orientation mechanisms seem to be more sensitive to the global geometry of the solute since the position of the bromide on the phenyl ring significantly affects the magnitude of $|\Delta\nu_{\text{O}}^{\text{average}}|$. This result could be related to the fact that these mechanisms are more sensitive to electrostatic intermolecular interactions, for which the position of the bromine atom plays an important role. This analysis of the results supports again the idea that the chiral discrimination and orientation phenomena do not follow the same laws and could be treated using different interaction mechanisms.

NMR study of 1-(2',6'-dideuterio-4'-methylphenyl)naphthalene (3): With regard to the MMC results, the spectral behaviour of **3** should be a priori very similar to that of **2** in spite of their stereochemical differences. Figure 7a shows some anisotropic $^2\text{H}\{-^1\text{H}\}$ NMR spectra of **3** recorded in the PBLG phase between 213 and 350 K (see also Figure SI-4 and SI-5a in the Supporting Information). Similarly to **2**, we observe a sharp quadrupolar doublet (linewidth < 5 Hz) at 302 K and above, while the coalescence phenomenon is reached at $T_c = (245 \pm 2)$ K. This T_c value is slightly lower than that for **2** because the difference in $\Delta\nu_{\text{O}}$ values for the C–D directions is now equal to 204 instead of 348 Hz. As before, the coalescence lineshape corresponds to the case in which the quadrupolar doublets have identical signs at low temperatures. The presence of two resolved doublets below

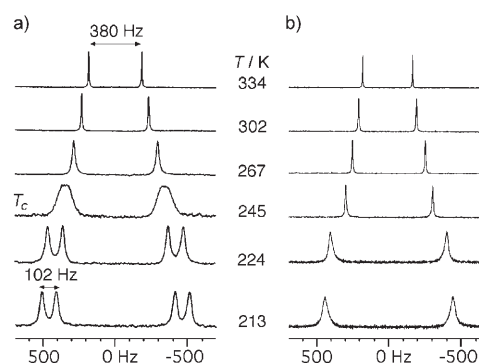


Figure 7. Experimental 61.4 MHz $^2\text{H}\{-^1\text{H}\}$ NMR spectra of **3** dissolved in a) the PBLG/ CHCl_3 phase and b) the PBG/ CHCl_3 phase at different temperatures as indicated. Note the difference in linewidth at 245 K.

T_c indicates two distinct averages for the orientation of the C–D directions ($S_{\text{C-D}}^{\text{pro-R}} \neq S_{\text{C-D}}^{\text{pro-S}}$). To confirm this result, we recorded the $^2\text{H}\{-^1\text{H}\}$ NMR spectra of **3** in the achiral phase PBG/ CHCl_3 over the same temperature range (see Figure 7b and SI-5b in the Supporting Information). A single doublet ($S_{\text{C-D}}^{\text{pro-R}} = S_{\text{C-D}}^{\text{pro-S}}$) was observed irrespective of the temperature. This last result shows that the two doublets observed at low T in PBLG do not originate from a particular reorientation phenomenon of the solute, but arise from the orientational non-equivalence of the C–D directions in the chiral mesophase. Thus we assess experimentally the enantiotopic character of these directions when the rotation is slow relative to the NMR timescale and so demonstrate that the molecular structure resulting from averaging of all rotamers has C_s symmetry.

By using an averaged value of $|\Delta\nu_{\text{O}}/2| = 102 \pm 5$ Hz, we calculated $k(T_c) = (226 \pm 11) \text{ s}^{-1}$ and $\Delta G^\ddagger(T_c) = (+48.6 \pm 0.5) \text{ kJ mol}^{-1}$ from Equations (5) and (6). By applying the procedure described above for **2**, the k values extracted from each simulated $^2\text{H}\{-^1\text{H}\}$ NMR spectrum were analysed using the Eyring's plot. The evolution of the average of the $\Delta\nu_{\text{O}}$ values (dashed lines) extrapolated from data measured in the slow regime correctly fits the evolution of $|\Delta\nu_{\text{O}}^{\text{average}}|$ (measured below and above T_c) from 213 to 305 K, but diverges slightly at higher temperatures (see Figure SI-4 in the Supporting Information). The discrepancy measured at 350 K is 38 Hz, that is, an error of around 10%. This effect is mainly related to the small number of points used for fitting data during the slow exchange regime (five points). As the temperature range used to evaluate k varies from 224 to 302 K, this divergence has only a small impact on the accuracy of k . Parameters derived from the Eyring's plot are given in Table 3. Once again the experimental ΔH^\ddagger value differs by less than 2 kJ mol^{-1} ($< 4\%$) from the value obtained by MMCs. The rotation rate calculated at 302 K ($k = 1.2 \times 10^4 \text{ s}^{-1}$) is very similar to the value found for **2**, thus confirming that the bromine atom in the *meta* position does not hinder rotation about the $\text{sp}^2\text{-sp}^2$ bond.

As in preceding examples, the evolution of $|\Delta\nu_{\text{O}}^{\text{average}}|$ for **3** dissolved in the PBLG and PBG phases can be fitted with good agreement by using Equation (8) ($\chi > 0.997$). Compari-

son of the results obtained in the two phases indicates that parameters C and E differ by less than 1 and 3%, respectively (see Table 2, entries 4 and 5). These minor discrepancies arise mainly from small differences in the sample preparation (slight changes in the composition) as well as in differences in the average degree of polymerisation (DP) of the polypeptides used (see Table 4). As in the case of **1**, the evolution of the difference of $\Delta\nu_Q$ values is linear below T_c . Again, we confirm the assumption that mechanisms for orientation and discrimination are not the same. In addition, it appears that the discrimination phenomenon could be seen as a simple perturbation of the orientation phenomenon. If this was not the case, the E fitting factors associated with the evolution of $|\Delta\nu_Q^A|$, $|\Delta\nu_Q^B|$ and $|\Delta\nu_Q^{\text{average}}|$ (in the PBG or PBLG phase) versus T should be very different. Except for the cases in which the angular terms $\theta_{C-D_i}^A$ and $\theta_{C-D_i}^B$ are rather close to the magic angle, the above statements could explain why the signs of the quadrupolar splittings for monodeuterated enantiomers or C–D enantiotopic directions are generally identical.

Experimentally, spectral discrimination of the enantiomeric rotamers (ϕ_1/ϕ_2 and ϕ_3/ϕ_4) was not observed in the spectra at low temperatures, even by recording the ^2H NMR spectrum at 200 K (not shown). Below this temperature, the sample starts to form a gel phase, thus preventing the use of PBLG as a weakly ordering liquid crystal with a low viscosity. This result is in accord with the MMCs since the height of the barrier between the most populated enantiomeric conformers, ϕ_1/ϕ_2 or ϕ_3/ϕ_4 , is only around 2 kJ mol^{-1} . Thus, if we assume that $|\Delta\Delta\nu_Q/2|$ could vary between 50 and 110 Hz, we can predict that the second coalescence phenomenon should be observed between 11.2 and 11.6 K! These temperatures are technically impossible to reach with current NMR probes and is evidently not applicable to a PBLG sample. Finally, note that the evolution of the spectra could also be explained by assuming a potential energy profile with only just two minima set at 90 and 270° , corresponding to a prochiral conformer of C_s symmetry.

NMR study of 1-(2'-deuterio-4'-methylphenyl)naphthalene (4): The evolution of the ^2H - $\{^1\text{H}\}$ NMR spectra (quadrupolar splitting, linewidths) for compound **4** versus T is very similar to that observed for **3** (see Figure SI-6 in the Supporting Information). The coalescence phenomenon is observed at $(245 \pm 2)\text{ K}$ and the average value of $|\Delta\Delta\nu_Q/2|$ measured below T_c (on three points) is equal to $(98 \pm 5)\text{ Hz}$ (instead of 102 Hz). This small deviation can be attributed to small differences in the sample composition, but also to the linewidths measured at T_c (around 25 Hz). By using these values, we obtain $k(T_c) = (218 \pm 10)\text{ s}^{-1}$ and $\Delta G^\ddagger(T_c) = (+48.4 \pm 0.5)\text{ kJ mol}^{-1}$. The activation parameters derived from the Eyring's plot analysis are listed in Table 3. Within experimental error, we can conclude that the activation parameters for **3** and **4** are identical. This means that the conformational dynamics are the same, or at least, the replacement of deuterium by the hydrogen atom does not modify the conformational behaviour of **4** compared with **3** suffi-

ciently to induce differences in the activation parameters larger than experimental error. The evolution of $|\Delta\nu_Q^{\text{average}}|$ versus T for **4** (dashed line) and **3** (continuous line) is plotted in Figure 8. As can be seen, small differences exist, in

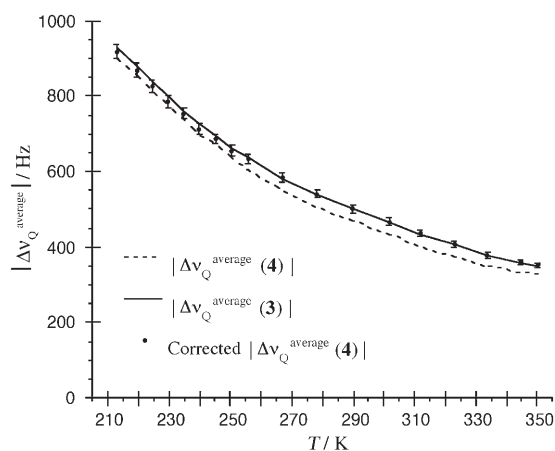


Figure 8. Comparison of $|\Delta\nu_Q^{\text{average}}(\mathbf{3})|$ and $|\Delta\nu_Q^{\text{average}}(\mathbf{4})|$ with and without corrections. Note the excellent fit between values of **4** (after correction) and **3**.

particular, at high temperatures. This effect primarily results from minor differences in the sample preparation or the macroscopic homogeneity of the phase. To correct these effects and obtain a more reliable comparison, a correction to $|\Delta\nu_Q^{\text{average}}(\mathbf{4})|$ can be applied by weighting each value with a parameter that is directly related to the liquid-crystalline phase. With this aim, we used the ^{13}C - ^1H dipolar coupling, $^1D_{\text{CH}}$, of the organic co-solvent (here, chloroform), which can be measured from the signals from ^{13}C satellites in the ^1H NMR spectra.^[15] The correction applied to $|\Delta\nu_Q^{\text{average}}(\mathbf{4})|$ is given by Equation (9).

$$|\Delta\nu_Q^{\text{corrected average}}(\mathbf{4})| = |\Delta\nu_Q^{\text{average}}(\mathbf{4})| \times \left| \frac{^1D_{\text{CH}}(\mathbf{3})}{^1D_{\text{CH}}(\mathbf{4})} \right| \quad (9)$$

Applying this correction harmonises the two sets of data. Quantitatively, differences of 3 and 2% in the C and E parameters, respectively, are found when the evolution of $|\Delta\nu_Q^{\text{average}}(\mathbf{3})|$ and $|\Delta\nu_Q^{\text{average}}(\mathbf{4})|$, after corrections, are fitted using Equation (8) (see Table 2, entries 4 and 8). From an orientational point of view, we have thus demonstrated that the origin of the discrimination of enantiomers of chiral molecules by virtue of isotopic substitution (H/D) is a consequence of the discrimination of enantiotopic C–D directions in related, prochiral molecules.

Influence of the co-solvent on the conformational dynamics:

As an extension of this study, we investigated the influence of the nature of the organic co-solvent on the orientational behaviour and the intramolecular dynamic processes of compounds **1** and **3**. For this purpose, we replaced chloroform by dichloromethane and recorded the ^2H NMR spectra

over the maximal temperature range 213–344 K. It is difficult to heat the PBLG sample in dichloromethane above 345 K owing to the boiling point of this co-solvent. Figure 9a

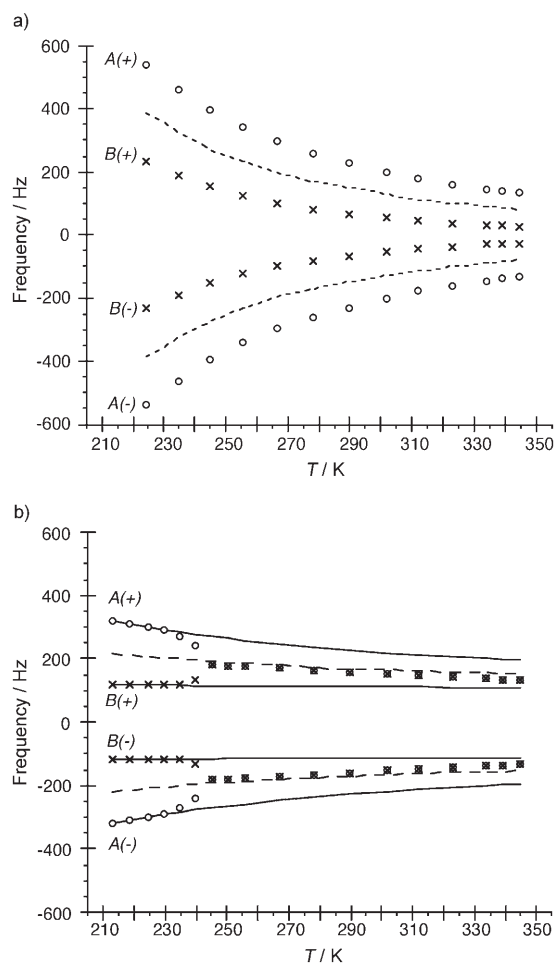


Figure 9. a) Evolution of the positive and negative components of doublets A (outer) and B (inner) of **1** in the PBLG/CH₂Cl₂ phase versus *T*. b) As for a), but for compound **3**. See the caption to Figure 6a for a definition of the curves and graphical points.

and 9b show the spectral evolution of the positive and negative components of the quadrupolar doublets of **1** and **3** as a function of temperature. In both cases, the global evolution of the $\Delta\nu_Q$ values is identical to that obtained when chloroform was employed as co-solvent. Thus for **3**, the coalescence effect is visible at (245 ± 2) K, while no effect is observed for **1** in the temperature range explored. By using the same procedure as described above for evaluating T_c for **1** dissolved in the PBLG/CHCl₃ phase and by setting ΔS^\ddagger to (-32 ± 2) J mol⁻¹ K⁻¹, we evaluate T_c and $\Delta G^\ddagger(T_c)$ to be 442.5 K and $+92.3$ kJ mol⁻¹, respectively. These data are similar to those obtained in PBLG/CHCl₃, thus reflecting the fact that the values of $|\Delta\Delta\nu_Q/2|$ are small and similar in both media at high temperatures. Similarly to preceding examples, the coalescence phenomenon for **3** is characterised by a single doublet with broad components and then by two

quadrupolar doublets below T_c . By using an average value of $|\Delta\Delta\nu_Q/2| = (106 \pm 5)$ Hz, we obtain $k(T_c) = (235 \pm 11)$ s⁻¹ and $\Delta G^\ddagger(T_c) = (+48.5 \pm 0.5)$ kJ mol⁻¹. As before, the evolution of the average of the $\Delta\nu_Q$ values extrapolated from data recorded in the slow exchange regime (dashed line) fits the evolution of $|\Delta\nu_Q^{\text{average}}|$ (measured below and above T_c) with an error < 5% between 213 and 305 K, but starts to diverge for temperatures above 305 K. At 340 K, the discrepancy is less than 40 Hz, that is, an error of 14%. The activation parameters derived from the Eyring's analysis are included in Table 3. Although the $\Delta G^\ddagger(T_c)$ value is slightly smaller than other $\Delta G^\ddagger(T_c)$ values, we estimate that the deviation between the activation parameters obtained in the PBLG/CHCl₃ and PBLG/CH₂Cl₂ phases is not sufficient to confirm that the nature of the co-solvent affects the dynamics of the compounds investigated here.

As before, the evolution of $|\Delta\nu_Q^{\text{average}}|$ for both compounds can be fitted using Equation (8). The *C* and *E* factors are listed in Table 2 (entries 2 and 6). The *E* factor, which reflects the decrease in the exponential function, is globally reduced by around 17% for **1** and 48% for **3** compared with values in the PBLG/CHCl₃ mesophase. These findings are consistent with the relative variations in $|\Delta\nu_Q^{\text{average}}|$, which are equal to 131% for **1** and 44% for **3** between $T_{\text{min}} = 224$ K and $T_{\text{max}} = 344$ K instead of 156 and 83% measured in the PBLG/CHCl₃ phase. Note also that there is only a small variation in $\Delta\nu_Q^B$ (Figure 9b), but it can still be fitted with an exponential function with a very small *E* factor, while the evolution of $\Delta\nu_Q^A$ shows a significant variation between T_{min} and T_{max} . The differential spectral evolution between the inner and outer doublets results from a different evolution of orientational behaviour between the enantiotopic C–D directions. This evolution, not observed for the other samples, is rather difficult to interpret because we probe only two directions of the five independent internuclear directions required to determine correctly Saupe's matrix.^[20,21] Put simply, we can assume that the C–D direction associated with $\Delta\nu_Q^B$ tends to reorient towards the magnetic field axis as *T* increases, thus balancing the global decrease in the molecular order parameters due to faster molecular motions.

Conclusion

Herein, we have demonstrated the robustness of ²H NMR spectroscopy in weakly ordering, chiral LCs for the investigation of the intramolecular dynamic processes of new diaryl atropisomers and related prochiral derivatives. This approach is a powerful method for calculating the kinetic and activation parameters of enantiomers or enantiotopic directions undergoing intramolecular conformational exchange because their spectral discrimination is much more efficient in an oriented polypeptide solvent compared with isotropic NMR methods dedicated to chiral analysis.

Beyond the advantages offered by this analytical method, the interpretation of these new experimental results has en-

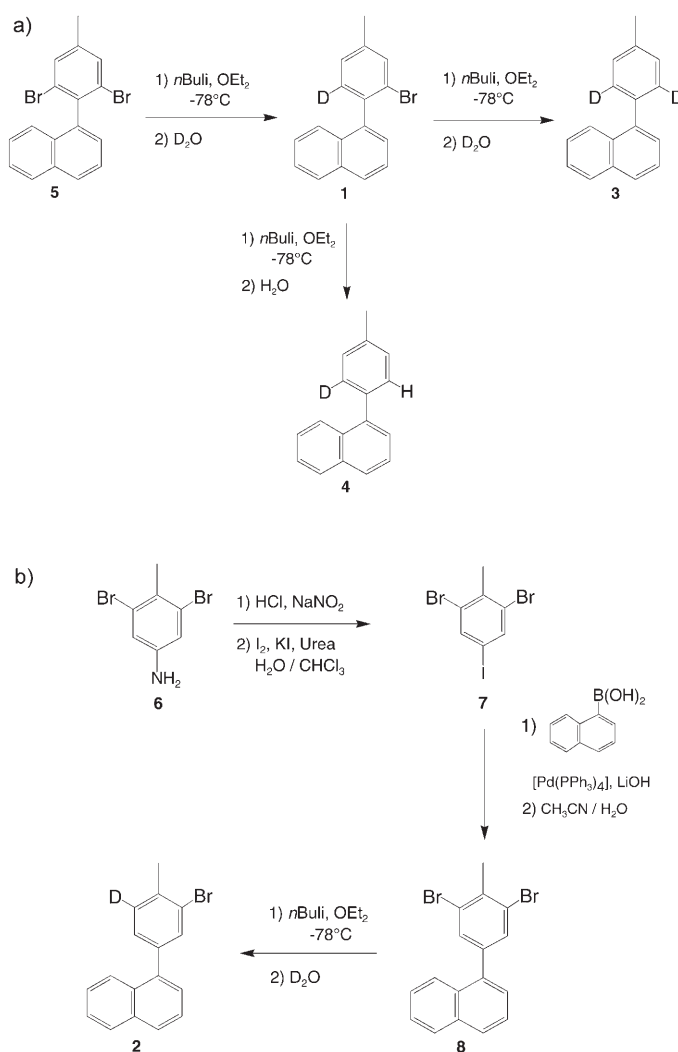
hanced our understanding of the orientation and chiral discrimination mechanisms in polypeptide LCs. First, we have demonstrated the excellent agreement between the theoretical evaluation of ΔH^\ddagger and experimental values extracted by NMR analysis using two different organic co-solvents. This result explicitly indicates that the intermolecular forces between the solute and the polypeptide oriented phase do not significantly influence the conformational interconversion process of molecules undergoing an intramolecular dynamic process (compared with an isolated molecule). The study of a possible deviation of activation parameters by changing the nature of polypeptide used (poly(γ -ethyl-L-glutamate) or poly(ϵ -carbobenzyloxy-L-lysine)) is currently underway. Secondly, in the temperature range explored, it appears that the evolution of $\Delta\nu_{\text{O}}$ values (in Hz) versus T (in K) can be fitted using an exponential function of the form $\Delta\nu_{\text{O}} = C \times \exp(-E/RT)$, whereas the evolution of the difference in $\Delta\nu_{\text{O}}$ values between enantiomers or two enantiotopic directions is linear. This situation suggests (at least for the compounds investigated here) that the mechanisms of orientation and discrimination could be treated separately because the contributions of shape recognition and purely electrostatic interactions differ in both mechanisms. Hence they can be seen as uncorrelated phenomena. With regard to these results, it seems that chiral discrimination might be seen as a simple perturbation of the orientation mechanism. This assessment is important for a better modelling of the PBLG system. It is also important to establish if the exponential function used for predicting the evolution of $\Delta\nu_{\text{O}}$ values versus T can be applied to a wide range of solutes. The question is now open.

Finally, this work points out a recurrent semantic problem between the communities of organic chemists and spectroscopists about the definition of the intrinsic stereoisomeric nature (chiral, prochiral)^[3] of a chemical species and how a molecule should be considered. This problem (already pointed out by several authors in various contexts^[16,45–47]) arises with the compounds investigated here, for which the stereoisomeric nature of the molecules can be discussed as a function of the temperature of the experiment. It raises the basic question as to whether the classical definition of stereoisomerism or pro-stereoisomerism should be imposed by the reality of synthetic chemistry, based either on the possibility of isolating a molecule^[3,45,46] or disposing of a chemical reaction able to synthesise enantiomers from a prochiral molecule,^[16,47] or the reality of the spectroscopic methods, which depend on the experimental conditions or the observational technique itself.^[46] With regard to these two points of view, the definition introduced by Eliel^[46] in which “a chemical species” is defined “as a molecule at or very near a minimum in a potential energy hypersurface” seems a priori to be more satisfactory because this concept is independent of the method of observation and experimental conditions as far as possible. Under this condition, two chemical species are identical when the interconverting energy barrier is less than RT and (stereo)isomeric when the barrier is higher. This definition offers the advantage of in-

volving no practical methodologies used in chemical laboratories, but to be related only to the stability scale of the various possible isomers of a given compound.

Experimental Section

Synthesis of deuterated compounds: Scheme 1a and 1b show the synthetic strategies leading to compounds **1–4**. The detailed description of the syntheses is reported in the Supporting Information.



Scheme 1. a) Synthesis of compounds **1**, **3** and **4**. b) Synthesis of compound **2**.

Practical aspects of NMR spectroscopy in oriented solvents: The PBLG and PBDG polymers are commercially available from Sigma Corp. The preparation of fire-sealed oriented samples can be found in references [14] and [15]. The samples were made by mixing the solute (ca. 15 mg), polypeptide (ca. 100 mg) and co-solvent (ca. 440 mg). The exact composition of each sample is listed in Table 4. The ^2H - $\{^1\text{H}\}$ NMR spectra were recorded on a 400 MHz Bruker Avance spectrometer equipped with a 5 mm QXO probe. The temperature was controlled by a BVT 3200 variable-temperature controller over the range of 200 (–73°C) to 350 K (+77°C). Note that the sample homogeneity is destroyed by boil-

Table 4. Composition of the liquid-crystalline NMR samples investigated.

NMR sample	Solute	Polymer	DP ^[a]	Co-solvent	Solute [mg] ^[b]	Polymer [mg] ^[b]	Co-solvent [mg] ^[b]	Amount of polymer [wt %]
1	1	PBLG	782	CHCl ₃	15	101	440	18.2
2	1	PBLG/PBDG	782/914	CHCl ₃	12	51+53	440	18.7
3	1	PBLG	782	CH ₂ Cl ₂	10	107	442	19.1
4	2	PBLG	782	CHCl ₃	12	101	440	18.3
5	3	PBLG	782	CHCl ₃	11	101	441	18.3
6	3	PBLG/PBDG	782/914	CHCl ₃	10	50+51	439	18.4
7	3	PBLG	782	CH ₂ Cl ₂	10	99	441	18.0
8	4	PBLG	782	CHCl ₃	11	99	442	18.0

[a] DP: average degree of polymerisation of the polypeptide used (PBLG and PBDG). [b] To an accuracy of ± 1 mg.

ing the co-solvent above 350 K for CHCl₃ and above 344 K for CH₂Cl₂. The temperature was calibrated using standard procedures. Mixtures were left for 10–15 min to equilibrate at the sample temperature before recording spectra. All 1D ²H NMR spectra were recorded with 1024 scans of 2048 data points. The tuning and matching of the deuterium coil were optimised at each temperature. The classical WALTZ-16 sequence was used to decouple protons (<0.4 W of power).

Acknowledgements

The authors are grateful to Prof. Dr. V. Schurig and Dr. O. Trapp for calculating the free energy of activation from the HPLC study. Also they cordially thank Dr. R. Paugam for stimulating discussions. O.L. and C.-A.F. acknowledge MNESER for a Ph.D. grant and the CNRS of Gif-sur-Yvette for their financial support, respectively.

- P. Llyod-Williams, E. Giralt, *Chem. Soc. Rev.* **2001**, *30*, 145–157, and references therein.
- M. Oki, *Top. Stereochem.* **1983**, *14*, 1–82, and references therein.
- A. L. Eliel, A. H. Wilen, *Stereochemistry of Organic Compounds*, Wiley, New York, **1994**.
- H. S. Gutowsky, D. W. McCall, C. P. Slichter, *J. Chem. Phys.* **1953**, *21*, 279–292.
- a) A. D. Bain, *Prog. Nucl. Magn. Reson. Spectrosc.* **2003**, *39*, 63–103, and references therein; b) S. Grilli, L. Lunazzi, A. Mazzanti, M. Pinamonti, *Tetrahedron* **2004**, *60*, 4451–4458; c) D. Casarini, C. Coluccini, L. Lunazzi, A. Mazzanti, *J. Org. Chem.* **2005**, *70*, 5098–5102.
- a) C. S. Johnson, *J. Magn. Reson., Ser. A* **1993**, *102*, 214–218; b) E. J. Cabrita, S. Berger, P. Bräuer, J. Kärgler, *J. Magn. Reson.* **2002**, *157*, 124–131; c) P. Thureau, B. Ancian, S. Viel, A. Thévand, *Chem. Commun.* **2006**, 200–202.
- R. Poupko, Z. Luz in *Encyclopedia of Nuclear Magnetic Resonance* (Eds.: G. M. Grant, R. K. Harris), Wiley, Chichester, **1996**, pp. 1783–1797, and references therein.
- Z. Luz in *Nuclear Magnetic Resonance of Liquid Crystals* (Ed.: J. W. Emsley), NATO, Dordrecht, **1985**, pp. 315–340.
- R. Poupko, Z. Luz, *J. Chem. Phys.* **1981**, *75*, 1675–1681.
- C. Boeffel, Z. Luz, R. Poupko, H. Zimmermann, *J. Am. Chem. Soc.* **1990**, *112*, 7158–7163.
- a) S. Ternieden, D. Muller, K. Muller, *Liquid Crystals* **1999**, *26*, 759–769; b) S. Ternieden, D. Zausser, K. Muller, *Liquid Crystals* **2000**, *27*, 1171–1182.
- M. E. Moseley, R. Poupko, Z. Luz, *J. Magn. Reson.* **1982**, *48*, 354–360.
- I. Canet, J. Courtieu, A. Loewenstein, A. Meddour, J.-M. Péchiné, *J. Am. Chem. Soc.* **1995**, *117*, 6520–6526.
- M. Sarfati, P. Lesot, D. Merlet, J. Courtieu, *Chem. Commun.* **2000**, 2069–2081.
- P. Lesot, M. Sarfati, J. Courtieu, *Chem. Eur. J.* **2003**, *9*, 1724–1745.
- a) C. Aroulanda, D. Merlet, J. Courtieu, P. Lesot, *J. Am. Chem. Soc.* **2001**, *123*, 12059–12066; b) P. Lesot, D. Merlet, M. Sarfati, J. Courtieu, H. Zimmermann, Z. Luz, *J. Am. Chem. Soc.* **2002**, *124*, 10071–10082.
- C. Aroulanda, M. Sarfati, J. Courtieu, P. Lesot, *Enantiomer* **2001**, *6*, 281–287.
- Note that the case of chiral, substituted cyclohexanes is very peculiar because the exchange rate between enantiomers can be determined without discriminating the enantiomeric forms. Indeed for these compounds, the interconversion between enantiomers also leads to the interconversion of diastereotopic directions (axial and equatorial bonds) that are nonequivalent in achiral LCs.
- P. Lesot, O. Lafon, C.-A. Fan, H. B. Kagan, *Chem. Commun.* **2006**, 389–391.
- C. Zannoni in *Nuclear Magnetic Resonance of Liquid Crystals* (Ed.: J. W. Emsley), NATO, Dordrecht, **1985**, pp. 1–31.
- J. W. Emsley, J. C. Lindon, *NMR Spectroscopy Using Liquid Crystal Solvents*, Pergamon Press, Oxford, **1975**.
- a) B. Halle, *Prog. Nucl. Magn. Reson. Spectrosc.* **1996**, *32*, 137–159; b) Z. Luz in *NMR of Ordered Liquids* (Eds.: E. E. Burnell, C. A. de Lange), Kluwer, Dordrecht, **2002**, pp. 419–448.
- M. H. Levitt, *Spin Dynamics*, Wiley, **2005**, Chichester, pp. 492–494.
- E. Gelerinter, Z. Luz, R. Poupko, H. Zimmermann, *J. Chem. Phys.* **1990**, *92–93*, 8845–8850.
- a) J. A. Pople, W. G. Schneider, H. J. Bernstein, *High Resolution NMR*, McGraw-Hill, New York, **1959**, pp. 218–230; b) G. Binsch, *Top. Stereochem.* **1968**, *3*, 97–192.
- H. Eyring, *Chem. Rev.* **1935**, *35*, 65–77.
- This approach is called the “coalescence temperature method”.
- M. J. S. Dewar, K. M. Dieter, *J. Am. Chem. Soc.* **1986**, *108*, 8075–8086.
- HyperchemTM, Professional 6.1, Hypercube, Inc, 1115 NN 4th street, Gainesville, Florida, 32601 (USA).
- a) R. F. Stewart, *J. Chem. Phys.* **1970**, *52*, 431–438; b) L. J. Sham, W. Kohn, *Phys. Rev.* **1965**, *140*, 1697–1705.
- a) K. L. Servis, R. L. Domenick, *J. Am. Chem. Soc.* **1986**, *108*, 2211–2214; b) S. Berger, H. Künzer, *Tetrahedron* **1983**, *39*, 1327–1329; c) G. S. Pawley, E. A. Yeats, *Acta Crystallogr. Sect. B* **1969**, *25*, 2009–2013.
- A. Meddour, I. Canet, A. Loewenstein, J.-M. Péchiné, J. Courtieu, *J. Am. Chem. Soc.* **1994**, *116*, 9652–9656.
- P. Lesot, O. Lafon, J. Courtieu, P. Berdagué, *Chem. Eur. J.* **2004**, *10*, 3741–3746.
- L. S. Bartell, *J. Am. Chem. Soc.* **1961**, *83*, 3567–3571.
- C. Canlet, D. Merlet, P. Lesot, A. Meddour, A. Loewenstein, J. Courtieu, *Tetrahedron: Asymmetry* **2000**, *11*, 1911–1918.
- a) P. Lesot, D. Merlet, A. Meddour, A. Loewenstein, J. Courtieu, *J. Chem. Soc., Faraday Trans.* **1995**, *91*, 1371–1375; b) A. Meddour, P. Berdagué, A. Hedli, J. Courtieu, P. Lesot, *J. Am. Chem. Soc.* **1997**, *119*, 4502–4508.
- a) I. Haller, *Prog. Solid State Chem.* **1975**, *10*, 103–118; b) H. Kneppel, V. Reiffenrath, *Chem. Phys. Lett.* **1982**, *87*, 59–62; c) M. L. Magnuson, B. M. Fung, J.-P. Bayle, *Liquid crystals* **1995**, *19*, 823–832.
- J. Israelachvili, *Intermolecular and Surface Forces*, Academic Press, San Diego, **1991**.
- a) J. Jeener, B. H. Meier, P. Bachmann, R. R. Ernst, *J. Chem. Phys.* **1979**, *71*, 4546–4553; b) C. Boeffel, Z. Luz, R. Poupko, A. J. Vega, *Isr. J. Chem.* **1989**, *29*, 283–296.
- In practice, we plot the two right sides of Equations (4) and (6) versus T_c and then determine the intersection point of the two plots.

- [41] This implies that the coalescence phenomenon cannot be reached at 350 K and hence the data derived from the MMCs are consistent with the NMR results. At 350 K, the value of ΔG^\ddagger determined from Equation (4) ($\Delta G^\ddagger = +84.7 \text{ kJ mol}^{-1}$) is too high compared with the value calculated with Equation (6) ($\Delta G^\ddagger = +70.9 \text{ kJ mol}^{-1}$).
- [42] a) V. Schurig, W. Bürkle, *J. Am. Chem. Soc.* **1982**, *104*, 7573–7580; b) F. Gasparrini, D. Misiti, M. Pierini, C. Villani, *Tetrahedron: Asymmetry* **1997**, *8*, 2069–2073; c) M. Jung, V. Schurig, *J. Am. Chem. Soc.* **1992**, *114*, 529–534.
- [43] W. Bürkle, H. Karfunkel, V. Schurig, *J. Chromatogr. A* **1984**, *288*, 1–14.
- [44] a) J. W. Emsley, P. Lesot, D. Merlet, *Phys. Chem. Chem. Phys.* **2004**, *6*, 522–530; b) J. W. Emsley, P. Lesot, J. Courtieu, D. Merlet, *Phys. Chem. Chem. Phys.* **2004**, *6*, 5331–5337.
- [45] K. Mislow, P. Bickart, *Isr. J. Chem.* **1977**, *17*, 1–6.
- [46] E. L. Eliel, *Isr. J. Chem.* **1977**, *17*, 7–11.
- [47] a) S. Fujita, *J. Am. Chem. Soc.* **1990**, *112*, 3390–3397; b) S. Fujita, *Tetrahedron* **2000**, *56*, 735–740.

Received: September 6, 2006
Published online: January 16, 2007